

Modeling of Rolling-Web AP-PECVD Reactors

Petr Hotmar, Hubert Caquineau, Nicolas Gherardi

Materials and Plasma Processes,
LABORATOIRE PLASMA ET CONVERSION D'ENERGIE, Toulouse

March 31, 2014

Outline

- 1 Model Description
- 2 Reactor Description
- 3 Optimization of Confinement Strength and Electrode Length

Modeling Objectives Achieved

- Optimize the AP-DBD reactor in terms of selectivity, deposition rate and product yield using a confining stream
- Examine deposition dynamics with modified T-injection and showerhead (limiting case of repeated confinements)
- Propose an injection head design with spatially uniform flow field of discharged gas using a CFD model
- Couple 1D and 2D fluid models of plasma discharge to examine plasma physics
 - In a decoupled model, time-dependent plasma equations are solved in 1D until periodic steady state is reached. The reaction source of dominant metastables $N_2 (A^3\Sigma_u^+)$ is subsequently coupled to the reaction chemistry of the 2D stationary model of the deposition reactor.

Model of Deposition Dynamics

- Incompressible, laminar flow of Newtonian solvent

$$\rho(\mathbf{u} \cdot \nabla) \mathbf{u} = \nabla \cdot \left[-\rho \mathbf{I} + \mu \left(\nabla \mathbf{u} + (\nabla \mathbf{u})^T \right) \right], \quad \rho \nabla \cdot \mathbf{u} = 0$$

- Transport of chemical species (HMDSO precursor, N_2 ($A^3\Sigma_u^+$) metastables and $[\text{Si}_2\text{O}]$ radicals)

$$\nabla \cdot (-D_i \nabla c_i) + \mathbf{u} \cdot \nabla c_i = R_i$$

Main Chemical Reactions

- 1 HMDSO + N_2 ($A^3\Sigma_u^+$) \rightarrow $[\text{Si}_2\text{O}]$ + Y_1 ($k_g = 4 \times 10^{-11} \text{ cm}^{-3}/\text{s}$, homogeneous reaction)
- 2 $[\text{Si}_2\text{O}]$ + 3 O \rightarrow Si_2O_4 (s) + Y_2 ($k_s = 1/4 \gamma c_c v_{th}$, surface reaction, oxidant excess)
- 3 HMDSO + N_2 ($A^3\Sigma_u^+$) \rightarrow HMDSO + N_2 ($k_q = k_g$, parallel quenching reaction)

Model Justification

Justifications of:

- Fluid model: low Knudsen number, $Kn = \lambda/H \sim 10^{-4} \ll 1$, where $\lambda = kT/(\sqrt{2}\pi d^2 p) \sim 10^{-7}$ m
- Decoupling: time scale separation between diffusive mass transfer and plasma discharge $\tau_{mass} = D_C/H \sim 1$ s
 $\gg \tau_{RF} \sim 10^{-4}$ s
- Decoupling: time scale separation between convective mass transfer and plasma discharge $\tau_{conv} = L/U > 10^{-3}$ s $> \tau_{RF}$
- Incompressibility: Mach number $Ma = U/c \sim 10^{-2} \ll 1$, with speed of sound c
- Dimensionality reduction: large geometrical aspect ratio
 $W \gg H$
- Laminar flow: Reynolds number $Re = UH/\nu \sim 10^2$, where ν is the kinematic viscosity

Outline

- 1 Model Description
- 2 Reactor Description
- 3 Optimization of Confinement Strength and Electrode Length

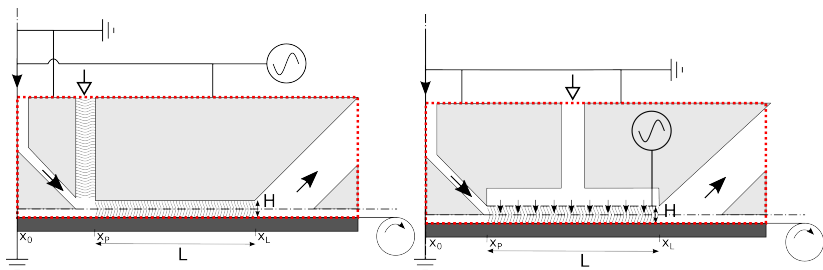
Reactor Design

- Deposition rate directly proportional to wall-normal flux of deposit species.
- Hydrodynamic confinement of precursor near depositing film → increase in selectivity and substrate-normal mass flux of reaction intermediates (radical species) due to their increased near-substrate concentration.
- Angled precursor injection serves to minimize recirculation zones and provide simple, uniform convective flow ($Pe \gg 1$).
- Injection head located close to substrate to minimize stray deposition and powder formation.
- Exhaust serves to remove by-products (incl. nano-powders) and reactive species. Angled to minimize turbulence (film inhomogeneity).

Design Limitations

- Model is, for the most part, constrained by the condition that the precursor concentration remains below a specified limit everywhere in the plasma zone. Even though relaxing this condition naturally results in increase in deposition rates, it may also induce filamentation due to increased quenching of N_2 metastables by HMDSO.
- At the expense of diluting the stream, the confining flow generates a high concentration layer within the gap cross section, located near the substrate.

Computational Domain – 2D cross-section



- Plasma source: $V_{RF} = 6 \text{ kV}$, $f = 5 \text{ kHz}$, $P = 1 \text{ W/cm}^2$
- Total gas flow rate $Q(N_2) = 5 \text{ slm}$
- Precursor concentration $c_{A0} = 50 \text{ ppm}$
- Confinement strength as a dilution factor $D = 1 - f_Q$, where f_Q is fraction of gas flow rate in precursor inlet
- Electrode length $L/H \in \langle 10..100 \rangle$, $H = 1 \text{ mm}$

Computational Domain – 3D

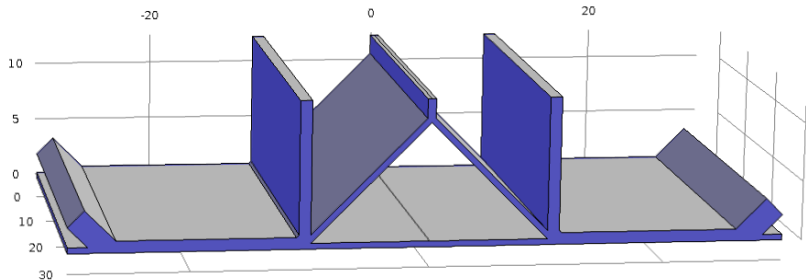


Fig.: A 3D sketch of the reactor for substrate width 3 cm.

Outline

- 1 Model Description
- 2 Reactor Description
- 3 Optimization of Confinement Strength and Electrode Length

Performance Criteria

Defining deposition selectivity S , rate v_N and yield Y_D ,

$$S \equiv \frac{\bar{v}_D - \bar{v}_D^S}{\bar{v}_D + \bar{v}_D^S} \in \langle -1, 1 \rangle, \quad (1)$$

$$v_N \equiv \frac{\bar{v}_D}{\bar{v}_D(D=0)}, \quad \text{where } \bar{v}_D^{(S)} = \frac{1}{L} \int_{x_P}^{x_L} v_D^{(S)}(x) dx, \quad (2)$$

$$Y_D = \frac{\int_0^H [c_A(x_P, y) - c_A(x_L, y) - c_C(x_L, y)] \mathbf{u} \cdot \mathbf{n} dy}{\int_0^H c_A(x_P, y) \mathbf{u} \cdot \mathbf{n} dy}, \quad (3)$$

where c_A and c_P are molar concentrations of precursor and product, respectively.

Selectivity

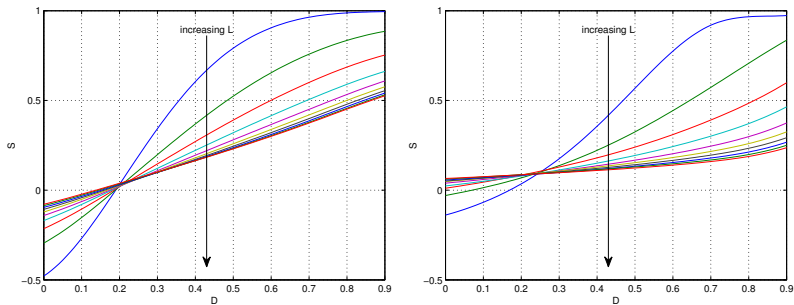


Fig.: The selectivity vs dilution factor. While the confining stream increases selectivity by suppressing stray deposition, its effect diminishes for increasing L . Left: T-injection. Right: Showerhead injection.

Deposition Rate

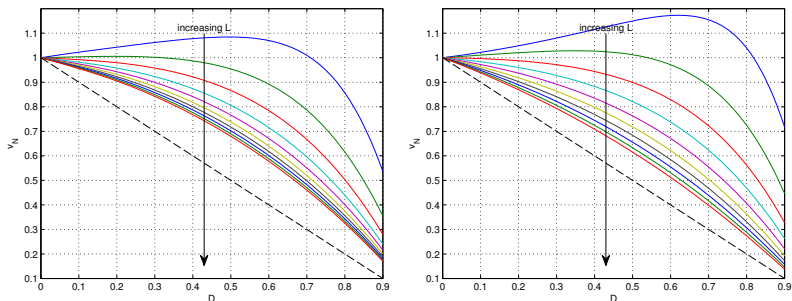


Fig.: The relative deposition rate vs dilution factor. The mass balance is favorable for short deposition regions. Left: T-injection. Right: Showerhead injection. The dashed line denotes an equivalently diluted system without the confining flow, for which $v_N = f_Q$.

Deposition Rate, Leveling the Playing Field

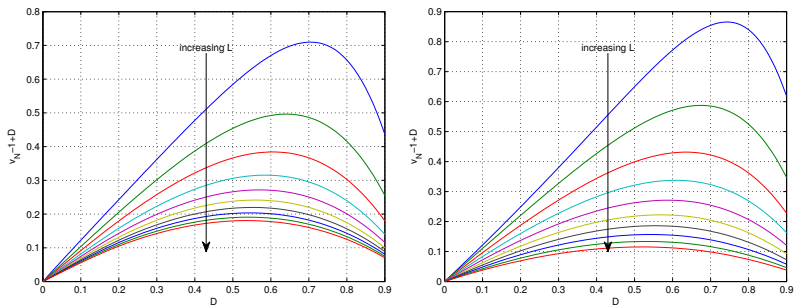


Fig.: Confinement efficiency as the difference between the relative deposition rate and the line $v_N = f_Q$, with the linear v_N dependence representing an equivalently diluted system without the confining flow. Left: T-injection. Right: Showerhead injection.

Example: Reference Deposition Rate Needed

So that we can: $v_N \rightarrow \bar{v}_D(Q, c_{A0}; D, L) \rightarrow \delta(v_w)$

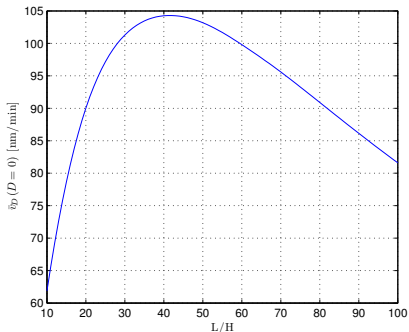


Fig.: The mean-integral deposition rate for given (Q, c_{A0}) without confinement ($D=0$, reference). For $L/H > 40$, the additional electrode length provides negligible contribution to the integral.

Example, Cont'd: Compensatory c'_{A0} Increase

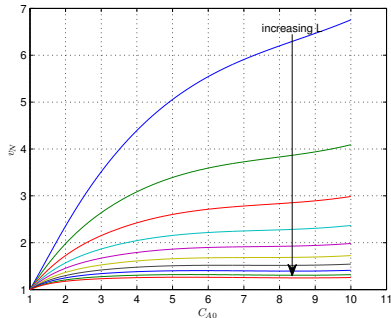
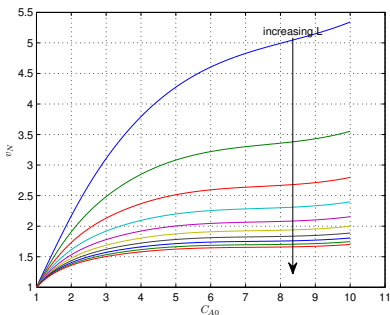


Fig.: The **deposition rate** vs c'_{A0} , with $C_{A0} = c'_{A0}/c_{A0} = 1/f_Q$. Left: T-injection. Right: Showerhead injection.

Example, Cont'd: Compensatory c_{A0} Increase

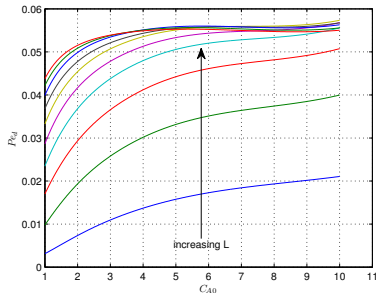
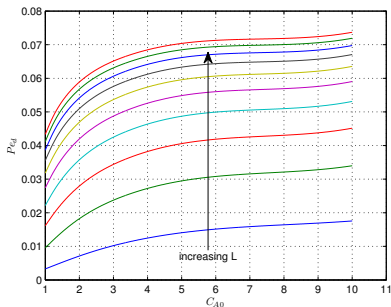


Fig.: The deposition Peclet number $Pe_d = \frac{\delta v_w}{D_{[Si_2O]}}$, with $\delta v_w = \bar{v}_D L$ and $D_{[Si_2O]} = 1.13 \times 10^{-5} \text{ m}^2/\text{s}$. For $D = \text{const}$, Pe_d is thus directly proportional to the **deposited height** $\delta = \frac{1}{v_w} \int_0^L v_D(x) dx$, or the product $\bar{v}_D L$, where $v_w = \text{const}$ is the substrate speed. Left: T-injection. Right: Showerhead injection.

Product Yield

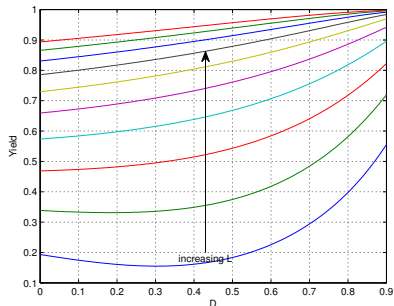
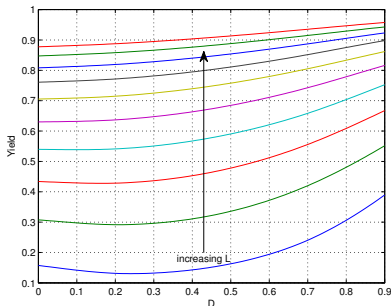


Fig.: Silica yield vs dilution factor. The dependence on D is gradually lost for long discharges as the gas residence time becomes sufficient for almost complete conversion of the precursor irrespective of internal re-distribution of flow rates within the reactor. Left: T-injection. Right: Showerhead injection.

Vector Optimization

A composite objective function β , based on a linear scalarization

$$\beta = \sum_{i=1}^3 w_i f_i(\mathbf{x}), \quad \sum_{i=1}^3 w_i = 1, \quad \mathbf{x}^* = \max_{\mathbf{x} \in \mathbf{X}} \beta(\mathbf{x}), \quad (4)$$

where $\mathbf{f} = (S, v_N, Y_D)$ are, respectively, the individual objective functions, normalized to $(0, 1)$ range and $\mathbf{w} = (w_S, w_V, w_G)$ is a corresponding weight vector. The solution vectors $\mathbf{x} = (D, L)$ are chosen from a set $\mathbf{X} = \mathbf{x} : \{0 \leq D < 1, 10 \leq L/H \leq 100\}$, with the feasible solution denoted by asterisk.

Vector Optimization

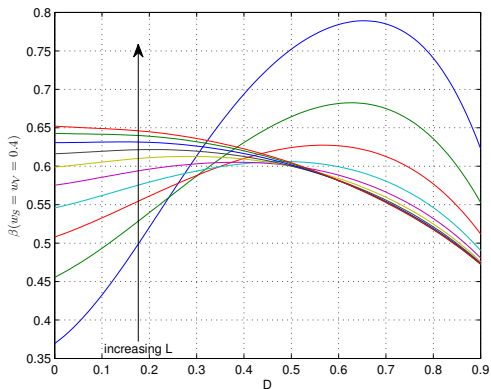


Fig.: For a specific weighting scheme of $w_S = w_V = 0.4$, we obtain $D^* = 0.65$ and $L^*/H = 10$, based on the objective function $\beta(D, L)$.
 T-injection.

Optimal Solutions

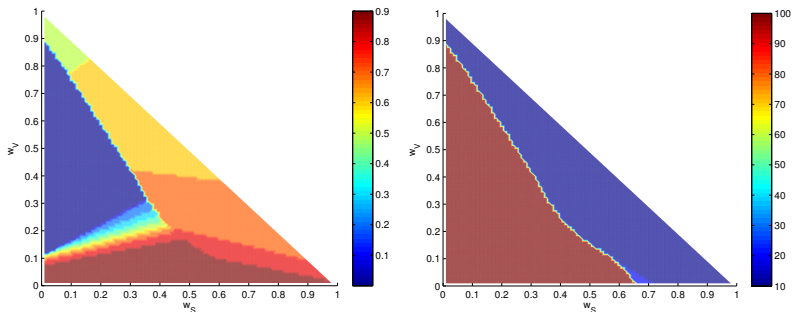


Fig.: Optimal solutions with selectivity, deposition rate and **product yield** as component objective functions. Left: Optimal dilution factor $D^* = D^*(w_S, w_W)$. Right: Optimal electrode length $L^* = L^*(w_S, w_W)$.

Sensitivity of Optimal Solutions to the Choice of Criteria

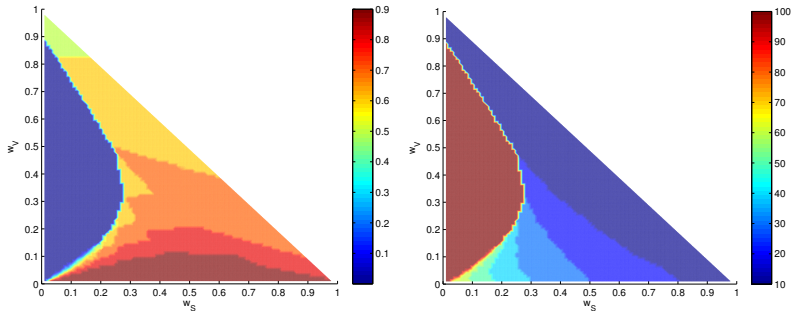


Fig.: Optimal solutions with selectivity, deposition rate and **precursor conversion** $\gamma_A = 1 - \frac{\int_0^H c_A(x_L, y) \mathbf{u} \cdot \mathbf{n} dy}{\int_0^H c_A(x_P, y) \mathbf{u} \cdot \mathbf{n} dy}$ as component objective functions.
 Left: Optimal dilution factor $D^* = D^*(w_S, w_W)$. Right: Optimal electrode length $L^* = L^*(w_S, w_W)$.

Conclusions

- **Selectivity** increases with D as the confining stream reduces stray deposition. The effect is, however, reduced for longer discharges due to interfacial diffusion which equalizes the cross-sectional concentration profile. T-injection preferred.
- Without compensatory increase in precursor concentration, the confinement increases **deposition rate** only for small L . For $L > L_{tres}$, the preferential deposition on the substrate (mass gain due to limited stray deposition) is unable to compensate for the mass loss of the precursor due to dilution. Showerhead preferred.
- The dependence of **product yield** on D is gradually lost for long discharges as the gas residence time becomes sufficient for almost complete conversion of the precursor irrespective of internal re-distribution of flow rates within the reactor.

Conclusions (cont'd)

- The domains of **optimal solutions** are dependent on the choice of optimization criteria. E.g. product yield criterion is more realistic, as it considers not only the precursor conversion ($A \rightarrow C$), but also the surface deposition of the reaction intermediate ($C \rightarrow D$), which can only occur over an additional diffusion length. We do not, however, consider powder formation due to unfavorable bulk reactions, which can be a limiting factor for long deposition chambers with long gas residence times. In such case the reactant conversion as an optimization criterion may be preferable.